Letter

TurboID-based proteomic profiling reveals proxitome of ASK1 and CUL1 of the SCF ubiquitin ligase in plants

Introduction

The SKP1-Cullin-F-box (SCF) complex is one of the best-studied E3 ubiquitin ligases in plants because of its critical roles in various signaling pathways (Lechner *et al.*, 2006; Sadanandom *et al.*, 2012; Stefanowicz *et al.*, 2015; Abd-Hamid *et al.*, 2020). The core components of SCF include Cullin 1 (CUL1) scaffold protein that interacts with SKP1 adaptor protein at the N-terminal, and E2-interacting RING-finger protein RBX1 at the C-terminal (Fig. 1a). The SKP1 interacts with interchangeable F-box receptor units that specifically recognize target substrates for ubiquitination and degradation by the 26S proteasome (Zheng & Shabek, 2017). Among the 21 SKP1-like (ASK) proteins in Arabidopsis, 19 exhibit significant structural similarity and are thought to be functionally redundant. Historically, studies have focused on ASK1 due to its prominent function as an adaptor in the SCF module, with higher steady-state levels of expression throughout the plant, particularly in proliferating tissues, compared with other ASK proteins (Porat *et al.*, 1998; Yang *et al.*, 1999; Zhao *et al.*, 1999; Gagne *et al.*, 2002; Risseeuw *et al.*, 2003). The Arabidopsis genome is predicted to encode hundreds of F-box proteins that target thousands of substrate proteins, but the majority remain uncharacterized and without known substrates (Abd-Hamid *et al.*, 2020). Interestingly, mammalian SKP1 has recently been shown to regulate the switch between autophagy and unconventional secretion (Li *et al.*, 2023), suggesting that its biological function extends beyond acting as an adapter protein within the SCF complex. Thus far, identifying E3 substrates has been challenging because substrates often interact weakly and transiently with the E3, and they are rapidly degraded and hence difficult to capture (Pierce *et al.*, 2009; Iconomou & Saunders, 2016). Although traditional methods such as affinity purification coupled to mass spectrometry (AP-MS), yeast-two hybrid (Y2H), and protein microarray screening have captured E3 substrates with some success, each has its own drawbacks (Harper & Tan, 2012; Iconomou & Saunders, 2016). AP-MS fails to capture weak and transient interactors, whereas Y2H is labor intensive, prone to false positives, and is a heterologous system. The recently developed proximity labeling (PL) approach to capture protein–protein interactions (PPI) *in vivo* overcomes many of the drawbacks of traditional approaches. For PL, a protein of interest (POI) is fused to a promiscuous biotin ligase. This ligase catalyzes biotin to a short-lived biotinoyl-5′-AMP, which can diffuse away from the ligase and react with amine groups on lysine residues of nearby proteins, typically within a radius of 10 nm (Kim & Roux, 2016; Qin *et al.*, 2021; Yang *et al.*, 2021). The biotinylated proximal interactomes (i.e. proxitomes) of the POI can be enriched using streptavidin-conjugated beads under stringent conditions followed by proteome identification through mass spectrometry (MS; Kim & Roux, 2016; Qin *et al.*, 2021; Yang *et al.*, 2021).

In this study, we utilized the TurboID biotin ligase, which is highly efficient at transferring biotin to proximal proteins in many organisms, including plants (Branon *et al.*, 2018; Mair *et al.*, 2019; Zhang *et al.*, 2019), to identify the SCF interactome in Arabidopsis. We uncovered the CUL1 and ASK1 proxitomes, providing insights into the functions of interactors in both conventional SCF-mediated signaling pathways and potentially noncanonical SCF-independent processes. Further investigation and analysis of the interactomes associated with ASK1 and CUL1 revealed novel partners involved in diverse biological processes within plants. The TurboID-based PL strategy detailed in this study can be expanded to identify targets belonging to other E3 families in plants. This expansion would enhance the repertoire of components within the ubiquitin-proteasome system and shed light on their pivotal roles in regulating a multitude of cellular processes.

Materials and Methods

Plant material, growth conditions, and agroinfiltration

Arabidopsis thaliana Col-0 and *Nicotiana benthamiana* plants were grown at 22°C in a growth chamber with a 16 h : 8 h light : dark photoperiod. The *Agrobacterium tumefaciens* (Agrobacterium) strain GV3101, containing pUBQ:TurboID-3xMyc-CUL1^{NTD}/gASK1 and pUBQ:Citrine-TurboID-3xMyc, was used to generate stable transgenic Arabidopsis lines by floral-dip method. For bimolecular fluorescence complementation (BiFC), co-immunoprecipitation (Co-IP), degradation, and ubiquitination assays, the GV3101 cultures carrying each construct were adjusted to an OD_{600} of 1. The appropriate cultures were combined in a 1 : 1 ratio and infiltrated into *N. benthamiana* with the infiltration buffer (10 mM $MgCl_2$, 10 mM MES pH 6, and 250 μM acetosyringone). MG132 (50 μM) was infiltrated 12 h before tissue collection.

Plasmid construction

For the TurboID experiment, the N-terminal domain (NTD) of AtCUL1 (1–380 aa), genomic DNA of AtASK1 (gASK1), and citrine were amplified via polymerase chain reaction. Both polymerase chain reaction fragments and vector were digested

New Phytologist

with *Xma*I and *Mlu*I enzymes to create pUBQ:TurboID-3xMyc-CUL1^{NTD}/gASK1 and pUBQ:citrine-TurboID-3xMyc constructs under the control of the Arabidopsis ubiquitin promoter (pUBQ) and nopaline synthase (NOS) terminator (Supporting Information Table S1a). The vector contains a kanamycin resistance gene for selection in *E. coli* and a BASTA resistance gene for selection in Arabidopsis. For BiFC, Co-IP, degradation, and ubiquitination assays, polymerase chain reaction fragments

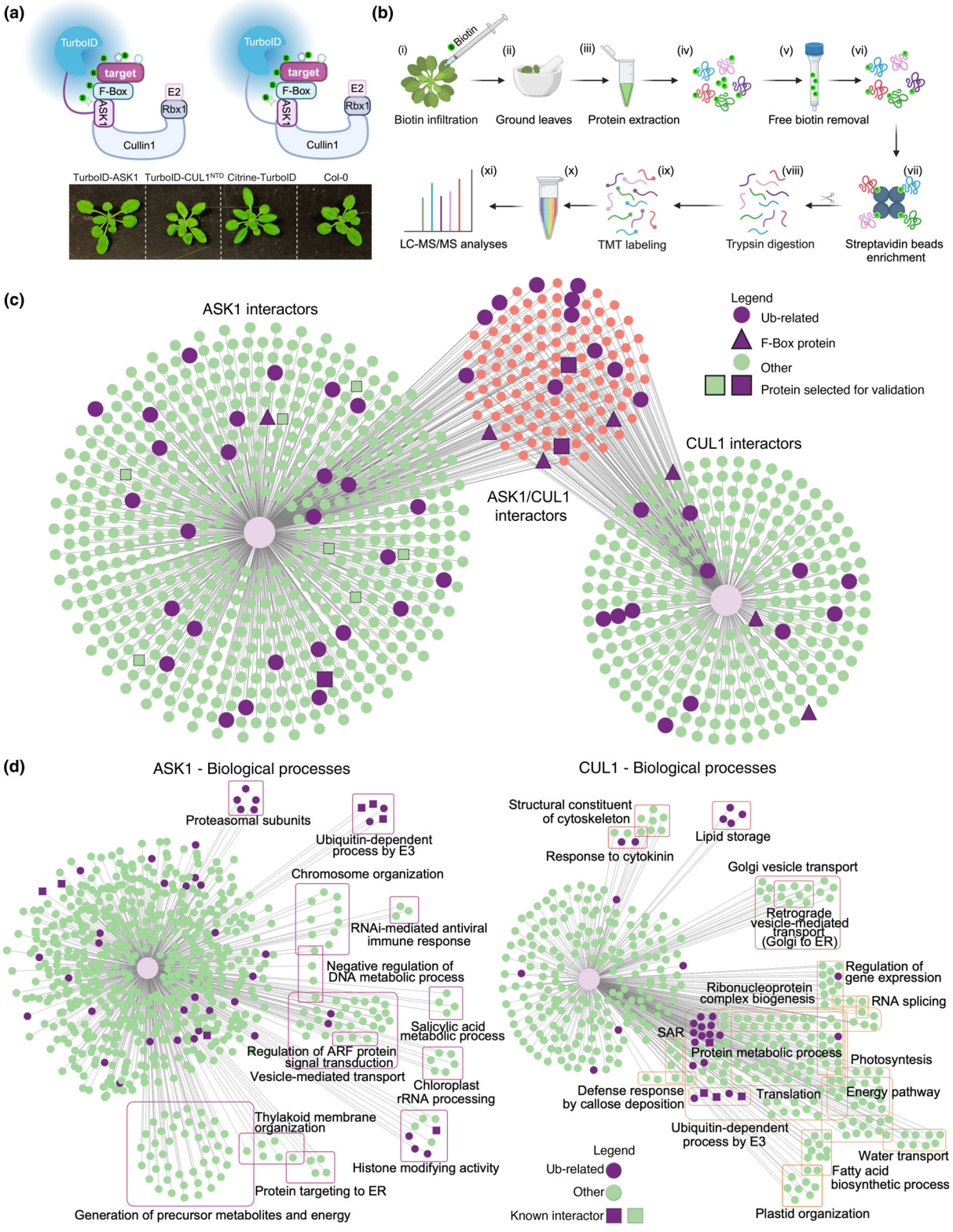

Fig. 1 Arabidopsis SKP1-Cullin-F-box (SCF) interactome network. (a) Schematic representation of TurboID fused to SCF subunit ASK1 (upper left panel) or SCF subunit Cullin 1 (CUL1) N-terminal domain ($CUL1^{NTD}$, upper right panel, shown as CUL1 for simplicity in the rest of the figure). The phenotype of Arabidopsis transgenic lines TurboID-ASK1, TurboID-$CUL1^{NTD}$, Citrine-TurboID, and Col-0 (lower panel). (b) Schematic of the workflow of TurboID proximity labeling process (i–xi). Leaves were infiltrated with biotin followed by 3-h incubation at room temperature (i); tissues were homogenized and lysed with RIPA lysis buffer (ii–iii), and free biotin was removed via desalting column (iv–v). The biotinylated proteins were enriched by streptavidin beads (vi–vii) follow by trypsin digestion (viii), TMT labeling (ix), and profiling using LC-MS/MS (x–xi). (c) Interactome network showing significant ASK1 (left network, green nodes), CUL1 (right network, green nodes), and ASK1/CUL1 (center network, orange nodes) interactors (q-value ≤ 0.1, fold change ≥ 1.23). Ubiquitin-related proteins are shown as purple nodes, F-box proteins are highlighted as triangle-shaped nodes, and proteins selected for further validation are square-shaped. (d) Individual ASK1 (left) and CUL1 (right) interaction networks where interactors with the same enriched ontology term were grouped (shaded boxes). Ubiquitin-related proteins are marked as purple circles. Images were generated using BioRender.com (a, b) and Cytoscape (c, d). ARF, ADP-ribosylation factor; ER, endoplasmic reticulum; SAR, systemic acquired resistance.

were amplified for the generation of constructs p35S:^{YC}3xHA-$CUL1^{NTD}$/gASK1 and p35S:targets-^{YN}3xMyc under the control of cauliflower mosaic virus 35S promoter (p35S) and NOS terminator using the Gateway cloning method (Invitrogen). Additionally, for the ubiquitination assay, the initial 76 amino acids of the coding sequence of *AtUBQ10* (AT4G05320) were amplified to create pUBQ:3xHA-Ubiquitin by infusion method (In-Fusion Snap Assembly cloning kit; Takara, San Jose, CA, USA). All primers used in this study are listed in Table S1(b).

TurboID sample preparation

For TurboID sample preparation for MS, an adapted version of the protocol from Zhang *et al.* (2019) was used with three biological replicates. Briefly, the stable transgenic lines were syringe-infiltrated with biotin and incubated under previously determined conditions. Leaves were collected in bulk, flash-frozen, and homogenized into a fine powder using mortar and pestle. For the total protein extraction, 1 g of homogenized tissue was aliquoted per replicate and rotated at 4°C for 30 min with RIPA lysis buffer (50 mM Tris pH 7.5, 500 mM NaCl, 1 mM EDTA, 1% NP40 (v/v), 0.1% SDS (w/v), 0.5% deoxycholate, 1 mM DTT, and protease inhibitor cocktail (Roche)). Tubes were subsequently centrifuged at 16 500 ***g*** for 10 min, and the soluble fraction was loaded into a Zeba™ Spin Desalting Columns (Thermo Fisher Scientific, Waltham, MA, USA), 7K MWCO to remove free biotin from the lysate. The concentration of the desalted protein samples was measured by the Bradford method (Kruger, 2009). To enrich biotinylated proteins, 200 µl Dynabeads™ MyOne™ Streptavidin C1 (Thermo Fisher Scientific) were prewashed with RIPA buffer and subsequently loaded with 6 mg desalted protein extract. Extract and beads were rotated at 4°C for 16 h and subsequently washed at room temperature with 1.7 ml buffer I (2% SDS), 1.7 ml buffer II (50 mM HEPES pH 7.5, 500 mM NaCl, 1 mM EDTA, 0.1% deoxycholic acid, and 1% Triton X-100), and 1.7 ml buffer III (10 mM Tris pH 7.4, 250 mM LiCl, 1 mM EDTA, 0.1% deoxycholic acid, and 1% NP40). The beads were then moved to 4°C, transferred to a new tube, and washed with 1.7 ml 50 mM Tris pH 7.5 and then 6× with 1 ml 50 mM ammonium bicarbonate. After the final wash, 30 µl bead resuspension was collected from each technical replicate for immunoblot analysis. Finally, the ammonium bicarbonate supernatant was removed, and the beads were flash-frozen in liquid nitrogen and stored at −80°C until LC-MS/MS analysis.

Sample prep and LC-MS/MS

Enriched samples were eluted from beads by incubation at 95°C for 10 min in 1× S-Trap lysis buffer (5% SDS, 50 mM TEAB, pH 8.5) supplemented with 12.5 mM biotin. Eluted samples were subjected to S-Trap sample processing technology (ProtiFi, Fairport, NY, USA), following the manufacturer's protocol. Samples were reduced in 2 mM TCEP, alkylated in 50 mM iodoacetamide (IAM), and digested into peptides at 37°C in one round of overnight incubation with 1 µg of trypsin and a second incubation of 4 h with 0.1 µg trypsin plus 0.1 µg Lys-C. Peptides were further desalted using SepPack C18 columns (Waters, Milford, MA, USA). Tandem Mass Tag (TMT; Thermo Fisher Scientific) labeling was performed on purified peptides from each sample as reported previously (Song *et al.*, 2020). TMT labeling reaction was stopped using 5% hydroxylamine, and the quenched samples were then pooled. Pooled samples were subjected to high pH fractionation using Pierce High pH Reversed-Phase Peptide Fractionation Kit (Thermo Fisher Scientific) following the manufacturer's instructions. The obtained eight fractions were further concatenated (pooled) as follows: Fraction 1 with Fraction 5, Fraction 2 with Fraction 6, Fraction 3 with Fraction 7, and Fraction 4 with Fraction 8. Samples were finally dried on a SpeedVac and resuspended in 0.1% Optima™ grade formic acid (Fisher) in Optima™ grade H_2O (Fisher). An injection volume of 20 µl, containing 1.2 µg from each concatenated fraction, was used for LC-MS/MS analysis.

Chromatography was performed on a Thermo UltiMate 3000 UHPLC RSLCnano. Peptides were desalted and concentrated on a PepMap100 trap column (300 µM i.d. × 5 mm, 5 µm C18, and 100 Å µ-Precolumn (Thermo Fisher Scientific)) at a flow rate of 10 µl min^{-1}. Sample separation was performed on a 200 cm Micro-Pillar Array Column (µPAC, Pharmafluidics) with a flow rate of *c.* 300 nl min^{-1} over a 150 min reverse phase gradient (80% ACN in 0.1% FA from 1% to 15% over 5 min, 15% to 20.8% over 20 min, from 20.8% to 43.8% over 80 min, and from 43.8% to 99.0% in 11 min, and kept at 99.0% for 5 min). Eluted peptides were analyzed using a Q-Exactive Plus high-resolution quadrupole Orbitrap mass spectrometer, which was directly coupled to the UHPLC. Data-dependent acquisition was obtained using the Xcalibur v.4.0 software in positive ion mode with a spray voltage of 2.3 kV and a capillary temperature of 275°C and an RF of 60. MS1 spectra were measured at a resolution of 70 000, an automatic gain control (AGC) of 3e6 with a maximum ion time of

100 ms and a mass range of 400–2000 *m/z*. Up to 15 MS2 were triggered at a resolution of 35 000. A fixed first mass of 115 *m/z*, an AGC of 1e5 with a maximum ion time of 50 ms, a normalized collision energy of 33, and an isolation window of 1.3 *m/z* were used. Charge exclusion was set to unassigned, 1, 5–8, and > 8. MS1 that triggered MS2 scans were dynamically excluded for 25 s.

Proteomics data and Gene Ontology analyses

Raw data were analyzed using MaxQuant v.2.1.0.0 (Cox & Mann, 2008). Spectra were searched, using the Andromeda search engine, against *Arabidopsis thaliana* TAIR10 annotation (Cox *et al.*, 2011; Berardini *et al.*, 2015). The proteome files were complemented with reverse decoy sequences and common contaminants by MaxQuant. Carbamidomethyl cysteine was set as a fixed modification while methionine oxidation and protein N-terminal acetylation were set as variable modifications. The sample type was set to 'Reporter Ion MS2' with 'TMT18plex' selected for both lysine and N-termini. TMT batch-specific correction factors were configured in the MaxQuant modifications tab (TMT Lot No.: XA338617). Digestion parameters were set to 'specific' and 'Trypsin/P;LysC'. Up to two missed cleavages were allowed. A false discovery rate, calculated in MaxQuant using a target-decoy strategy, < 0.01 at both the peptide spectral match and protein identification level was required (Elias & Gygi, 2007). The match between runs feature of MaxQuant was not utilized. ASK1 and CUL1^{NTD} significant interactors were assessed using the TMT-NEAT R pipeline with the poissonseq R package (Clark *et al.*, 2021; Li *et al.*, 2012). A *q*-value < 0.1 and $\log_2$(fold change) > 0.3 were used as cutoffs for designating enrichment. Significant enrichment of Biological Processes (BPs) and cellular components among ASK1 and CUL1^{NTD} interactors was determined using the ClueGO Cytoscape plugin on Cytoscape v.10.0.1 (Shannon *et al.*, 2003; Bindea *et al.*, 2009). Terms with *P*-value < 0.05 were selected as enriched. Network visualization of interactors was made on Cytoscape. Ubiquitin-related proteins were obtained from manual curation of known proteins, plus any protein that was part of the following BPs: ubiquitin-dependent protein catabolic process (GO:0006511), proteasomal protein catabolic process (GO:0010498), or protein ubiquitination (GO:0016567). The BP terms: Proteasome activating activity, SCF-dependent proteasomal ubiquitin dependent catabolic process, and Generation of precursor metabolites and energy, are represented as Proteasomal subunits, ubiquitin dependent processes, and Energy pathways, respectively. Reported ASK1/CUL1 interactors were obtained from literature mining and Arabidopsis Interactome Viewer in The Bio-Analytics Resource for Plant Biology (BAR; Geisler-Lee *et al.*, 2007; Waese & Provart, 2016). This mining tool includes searching on IntAct, BioGrid, and STRINGdb.

Immunoblotting and co-immunoprecipitation assay

Proteins were separated using self-made 10–13% SDS-PAGE gels. Total plant extracts containing the POI were prepared and subjected to SDS-PAGE and then transferred to Immobilon-P PVDF membrane (Millipore) using a wet transfer system (Bio-Rad). Membranes were blocked with 5% fat-free milk in 0.01% TBST (for Streptavidin-HRP in 2.5% BSA) for 1 h at room temperature, followed by incubation with appropriate antibodies at 4°C overnight. The next day, the membrane was washed three times with 0.1% TBST, followed by a 1-h incubation with a secondary antibody. Antibodies used in this study include mouse anti-c-Myc (Santa Cruz, Dallas, TX, USA, catalog no.: sc-40; 1 : 5000 dilution), Streptavidin-HRP (Abcam, Eugene, OR, USA, catalog no.: ab7403; 1 : 10000 dilution), anti-HA-HRP (Roche, catalog no.: 12013819001; 1 : 5000 dilution), and anti-Myc-HRP (Sigma-Aldrich, catalog no.: SAB4200742; 1 : 5000 dilution). Bands were visualized using SuperSignal™ West Pico PLUS Chemiluminescent Substrate (Thermo Fisher Scientific) and/or SuperSignal™ West Femto Maximum Sensitivity Substrate (Thermo Fisher Scientific). Chemiluminescent signals were acquired using a ChemiDoc™ Touch Imaging System (Bio-Rad). The band signal intensity was quantified using the ImageLab (Bio-Rad).

Co-IP assay of CUL1^{NTD} and ASK1 with their targets was conducted as described previously (Liang *et al.*, 2020). In brief, *N. benthamiana* leaves co-infiltrated with the targets were collected and ground into a fine powder using liquid nitrogen. The leaf powder was transferred into a 2-ml Eppendorf tube, and 2.5× (g ml^{-1}) Co-IP extraction buffer (25 mM Tris–HCl pH 7.5, 1 mM EDTA, 150 mM NaCl, 10% Glycerol, 0.15% NP-40, 10 mM DDT, 1 mM PMSF, 2% PVPP (Polyvinylpolypyrrolidone) and protease inhibitor cocktail (Roche)) was added. The mixture was vortexed and inverted for 30 min, followed by a high-speed spin down for 10 min at 4°C. Antibody-conjugated beads were pre-equilibrated with washing buffer (extraction buffer without 2% PVPP), and then, plant extracts were rotated at 4°C for 3 h. The supernatant was removed using a magnetic rack, and the beads were washed three times with a washing buffer. The dry beads were then added to a 2× sample buffer and boiled for 5 min for subsequent immunoblot analysis. All uncropped gels and loading controls are presented in Fig. S1.

Confocal microscopy

Nicotiana benthamiana leaves were imaged using a Zeiss LSM 980 with an Airyscan2. Leaf sections measuring 1 × 1 cm were excised, positioned distally to the syringe infiltration site. All images within the figure were acquired under consistent confocal settings and processed using Fiji software. Citrine and Chl fluorescence were observed under 514 and 693 nm, respectively.

Proteasome-dependent degradation and ubiquitination assays

The *N. benthamiana* leaves infiltrated with targets were infiltrated with MG132 (50 μM), 12 h before collection. The collected leaves were ground into a fine powder using liquid nitrogen. 2.5× (g ml^{-1}) 2× sample buffer was directly added to the powder, followed by boiling for 5 min for immunoblot analysis. For the ubiquitination assay, Agrobacterium strain GV3101 containing p35S:targets^{YN}-3xMyc and pUBQ:3xHA-UBQ10 was

co-infiltrated into *N. benthamiana*. Thirty-six hours later, 50 μM MG132 was infiltrated, and leaf tissue was collected at 48 h. The Co-IP assay was performed as described above. The target proteins were enriched using Myc-conjugated magnetic beads and anti-HA for ubiquitination analysis by immunoblot.

Results

In the SCF complex, CUL1 associates with ASK1, and ASK1 recruits F-box proteins along with their target substrates for degradation (Fig. 1a). Therefore, we used Arabidopsis CUL1 and ASK1 as bait to capture SCF targets under normal growth conditions (Fig. 1a). To that end, we fused 3xMyc epitope tag and TurboID to the N-terminus of ASK1 (TurboID-ASK1) under the control of Arabidopsis ubiquitin promoter (pUBQ) and NOS terminator (Fig. 1a, top panels and Fig. S2a). Similarly, we constructed the NTD of CUL1 fused to TurboID-3xMyc (TurboID-CUL1^{NTD}). The CUL1^{NTD} was designed as described previously (Zheng *et al.*, 2002), to enrich and stabilize E3 targets by eliminating the CUL1-RBX1 region and subsequent recruitment of E2 ubiquitin-conjugating enzymes. As a control to account for background biotinylation, we used Citrine fluorescent protein fused to TurboID-3xMyc (Citrine-TurboID; Fig. S2a). These constructs were transformed into Arabidopsis Col-0 plants, and T3 homozygous lines were selected and validated (see the Materials and Methods section for details). At 4 weeks, TurboID-CUL1^{NTD}, TurboID-ASK1, and Citrine-TurboID transgenic lines appear phenotypically similar to wild-type (WT) Col-0 plants (Fig. 1a, bottom panels). The expression of TurboID fusion proteins in these lines was confirmed by immunoblot analysis (Fig. S2b–d). Among different methods, we tested for biotin application, syringe infiltration of biotin into leaves delivered biotin more efficiently and caused less tissue damage compared with vacuum infiltration and submersion in the biotin solution. Subsequent time course experiments and immunoblotting with streptavidin-conjugated HRP revealed that 50 μM biotin infiltration and incubation for 3-h postinfiltration at room temperature was sufficient for efficient labeling activity for all tested TurboID fusions (Fig. S2b–d). In WT Col-0 plants, infiltration of 200 μM biotin followed by incubation at 3 h at room temperature resulted in detection of very few biotinylated proteins (Fig. S2b,d, last lane). These results indicate that biotin-labeled proteins were observed exclusively in the transgenic lines expressing TurboID fusions.

To identify ASK1 and CUL1^{NTD} proximal proteins, we performed affinity purification of biotinylated proteins in three replicates (Fig. 1b; see the Materials and Methods section for details). Immunoblot analysis confirmed the successful enrichment of biotinylated proteins on beads (Fig. S2e). The biotinylated proteins bound to streptavidin beads were eluted using boiling SDS supplemented with 12.5 mM biotin. Eluted proteins were cleaned and digested. The resulting peptides were labeled with distinct TMT and analyzed by liquid chromatography–tandem mass spectrometry (LC-MS/MS; Fig. 1b). Our analysis identified a total of 2361 proteins and quantified 2241 (Table S2a–c). Biological replicates taken from plants expressing the same transgene showed a high Pearson correlation (*c.* 0.99; Fig. S3). Among the identified proteins, 705 and 404 were considered ASK1 and CUL1 interactors, respectively, based on the threshold of q-value ≤ 0.1 and fold change (ASK1/Citrine or CUL1/Citrine) ≥ 1.23 (Fig. 1c; Table S2d,e). Comparison between ASK1 and CUL1 interactors identified 120 common interactors (Fig. 1c; Table S3). The unique and common interactors include F-box proteins and other ubiquitin-related proteins (Fig. 1c; Tables S4, S5).

To understand the functional significance of enriched ASK1 and CUL1 interactions, we performed Gene Ontology (GO) BP enrichment analysis. A large number of CUL1 interactors were related to protein metabolic process and gene expression categories (i.e. RNP biogenesis, translation, and RNA splicing; Fig. 1d; Table S6). Conversely, ASK1 interactors were, mostly, spread in smaller groups across various significantly enriched BPs. For both datasets, the BP term 'SCF-dependent proteasomal ubiquitin-dependent protein catabolic process' (referred to as ubiquitin-related) was enriched (Fig. 1d; Table S6). To further characterize ASK1/CUL1 interactors from our list, we compiled a list of F-box proteins and proteins related to ubiquitination or proteasomal activity and looked for them in our proxitome dataset. Statistical testing showed significant enrichment of 'ubiquitin-related' proteins among ASK1 interactors (P-value = 0.0014), and CUL1 interactors (P-value = 0.0015, hypergeometric test; Table S7).

In the CUL1^{NTD} interactors, previously described F-boxes were among the most highly enriched. These include AUXIN SIGNALING F-BOX 3 (AFB3), CORONATINE INSENSITIVE 1 (COI1), F-BOX AND LEUCINE RICH REPEAT DOMAINS CONTAINING PROTEIN (FBD), CONSTITUTIVE EXPRESSER OF PR GENES 1 (CPR1), and SLOW MOTION (SLOMO) (Dharmasiri *et al.*, 2005; Xu *et al.*, 2002; Kuroda *et al.*, 2012; Gou *et al.*, 2009; Lohmann *et al.*, 2010; Table S5a). The F-boxes AFB2, AFB5, and FBD were most highly enriched in the ASK1 data set, as well as PHYTOCHROME A (PhyA), MAPK/ERK KINASE KINASE 1 (MEKK1), PIN-FORMED 1 (PIN1), EXOCYST SUBUNIT EXO70 FAMILY PROTEIN A1 (EXO70A1), MITOGEN-ACTIVATED PROTEIN KINASE KINASE 5 (MKK5), and OLEOSIN 1 (OLE1) (Table S5b), which have been previously demonstrated to undergo 26S proteasome-mediated degradation but were not specifically shown to be targeted by SCF E3 complex (Clough & Vierstra, 1997; Dharmasiri *et al.*, 2005; Nakagami *et al.*, 2006; Nguyen *et al.*, 2013; Traver & Bartel, 2023).

Given that 77 proteins in our dataset are explicitly grouped under ubiquitin-related proteins and our dataset also included 12 previously described interactors of ASK1 and CUL1 (Fig. 1c; Table S5), we postulated that our ASK1 and CUL1^{NTD} TurboID fusions captured a mixture of SCF substrates and F-boxes, most of which are novel. To test whether these are bona fide target substrates of the SCF E3 ligase, we selected a dozen proteins for further *in planta* validation (Table S8). First, we performed a BiFC assay to confirm the interactions using *Agrobacterium*-mediated transient expression in *N. benthamiana* followed by confocal microscopy. For this, we co-expressed candidate interactors fused to the N-terminal 155 amino acid residues of citrine (candidate interactors^{YN}) and CUL1^{NTD} or ASK1 fused to the C-terminal

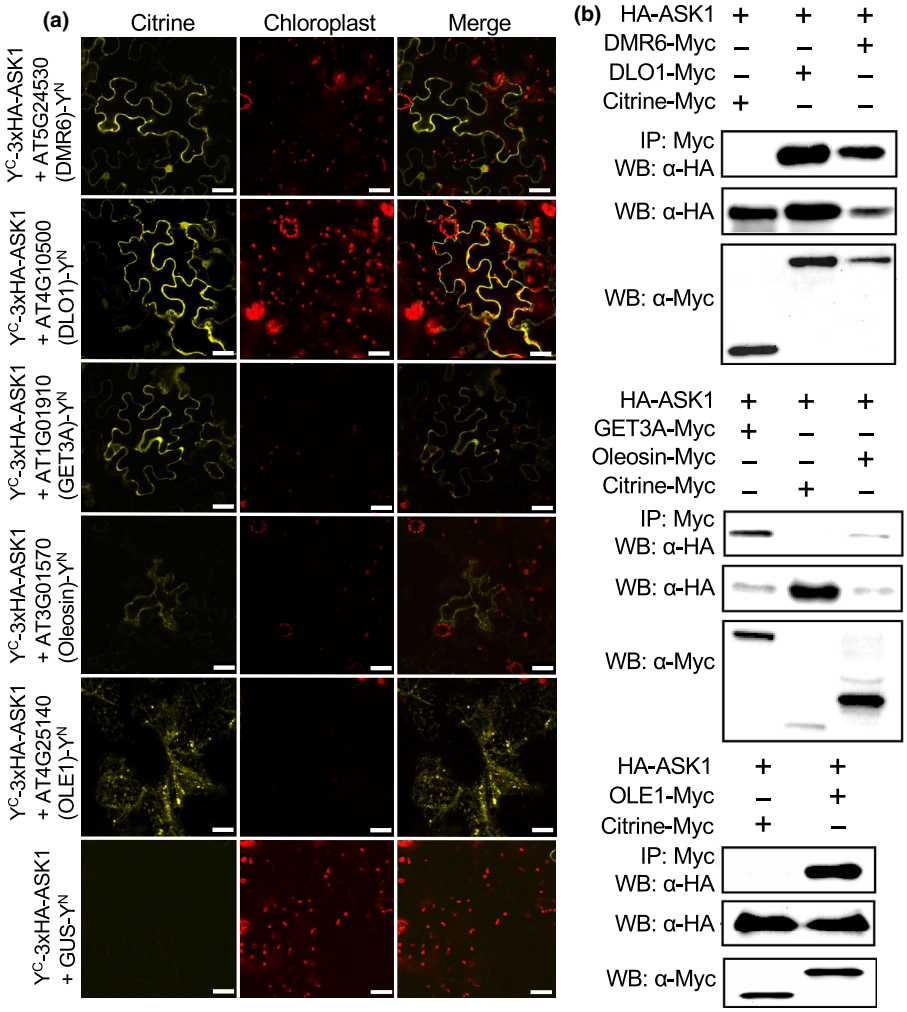

Fig. 2 Validation of ASK1 interacting targets. (a) Bimolecular fluorescence complementation (BiFC) analysis of the interaction between ASK1 and selected target proteins: DMR6 (AT4G10500), DLO1 (AT5G24530), GET3A (AT1G01910), Oleosin (AT3G01570), and OLE1 (AT4G25140). ASK1 was fused to the C-terminal fragment of citrine (^{YC}ASK1) and the interacting target proteins were fused to the N-terminal fragment of citrine (target proteins^{YN}). Constructs were co-infiltrated into *Nicotiana benthamiana* plant leaves, with GUS^{YN} as the negative control. Confocal microscopy was performed 36 hours postinfiltration (hpi). Reconstituted citrine fluorescence indicates a positive interaction. Bars, 30 μm. (b) Co-immunoprecipitation (Co-IP) analysis demonstrating the interaction between ASK1 and the target proteins. Agrobacterium harboring 3xHA-tagged ASK1 (HA-ASK1) and 3xMyc-tagged target proteins (target-Myc) or citrine-Myc control were co-infiltrated into *N. benthamiana* plant leaves. At 36 hpi, 50 μM MG132 was infiltrated, and 12 h later, leaf tissues were harvested. Proteins were immunoprecipitated (IP) with agarose beads conjugated with Myc antibody followed by Western blot (WB) with HA antibody (top panel in each group).

156–239 amino acid residues of citrine (^{YC}ASK1 or ^{YC}CUL1^{NTD}). Co-expression of ^{YC}ASK1 with DMR6^{YN} (DOWNY MILDEW RESISTANT 6), DLO1^{YN} (DMR6-LIKE OXYGENASE 1), GET3A^{YN} (GUIDED ENTRY OF TAIL-ANCHORED PROTEIN 3A), Oleosin^{YN}, OLE1^{YN}, CMPG2^{YN} (CYS, MET, PRO, AND GLY PROTEIN 2), MKK5^{YN}, MEKK1^{YN} (MAPK/ERK KINASE KINASE 1), RBR1^{YN} (RETINOBLASTOMA-RELATED PROTEIN 1), FBD^{YN}, or PhyA^{YN}, reconstituted citrine fluorescence, but not when ^{YC}ASK1 co-expressed with GUS^{YN} control (Figs 2a, S4a). Co-expression of ^{YC}CUL1^{NTD} with PhyA^{YN}, Oleosin^{YN}, or GET3A^{YN} reconstituted citrine fluorescence, but not when ^{YC}CUL1^{NTD} co-expressed with GUS^{YN} control (Fig. S4a). Although EXO70A1 (AT5G03540.2) was identified as an interactor in our PL, we were unable to see reconstituted citrine fluorescence in the BiFC assay (Fig. S4a). These results indicated that 11 out of the 12 tested proteins interacted in the BiFC assay *in planta*.

Next, we selected a subset of confirmed BiFC interactors as potential novel SCF substrates for the Co-IP assay. To that end, 3xMyc epitope tag fused DMR6, DLO1, GET3A, Oleosin, and OLE1 were each co-expressed in *N. benthamiana* with 3xHA tag fused to ASK1. Myc-conjugated beads were utilized for the pull-down, followed by immunoblotting with HA antibodies. Immunoblot analysis confirmed a successful pull-down of HA-ASK1 by MYC-tagged targets from the plant extract (Fig. 2b). Myc-tagged citrine served as a control and did not pull-down HA-tagged ASK1 (Fig. 2b). Additionally, in a reciprocal experiment, Myc-tagged GET3A and Oleosin were also pulled down by HA-tagged CUL1^{NTD} using HA-conjugated beads (Fig. S4b).

To assess whether the interacting candidates are indeed SCF E3 ubiquitin ligase target substrates that undergo ubiquitination and proteasomal degradation, HA-tagged ubiquitin was co-expressed with Myc-tagged DMR6, DLO1, OLE1, Oleosin, GET3A, and PhyA in *N. benthamiana*. Myc-conjugated beads were used to pull down, followed by immunoblot using anti-HA antibodies. Immunoblot analysis showed high molecular weight polyubiquitin conjugates for each of the tested substrates (Fig. 3a). Since the fate of SCF's polyubiquitinated substrates is typically proteasomal degradation, we tested the effect of MG132, a proteasome inhibitor (Teicher & Tomaszewski, 2015) on the degradation of Myc-tagged substrates. Remarkably, protein levels for all tested substrates were significantly elevated in the presence of MG132 (Fig. 3b), further corroborating that the identified interacting proteins serve as bona fide SCF ubiquitin ligase substrates.

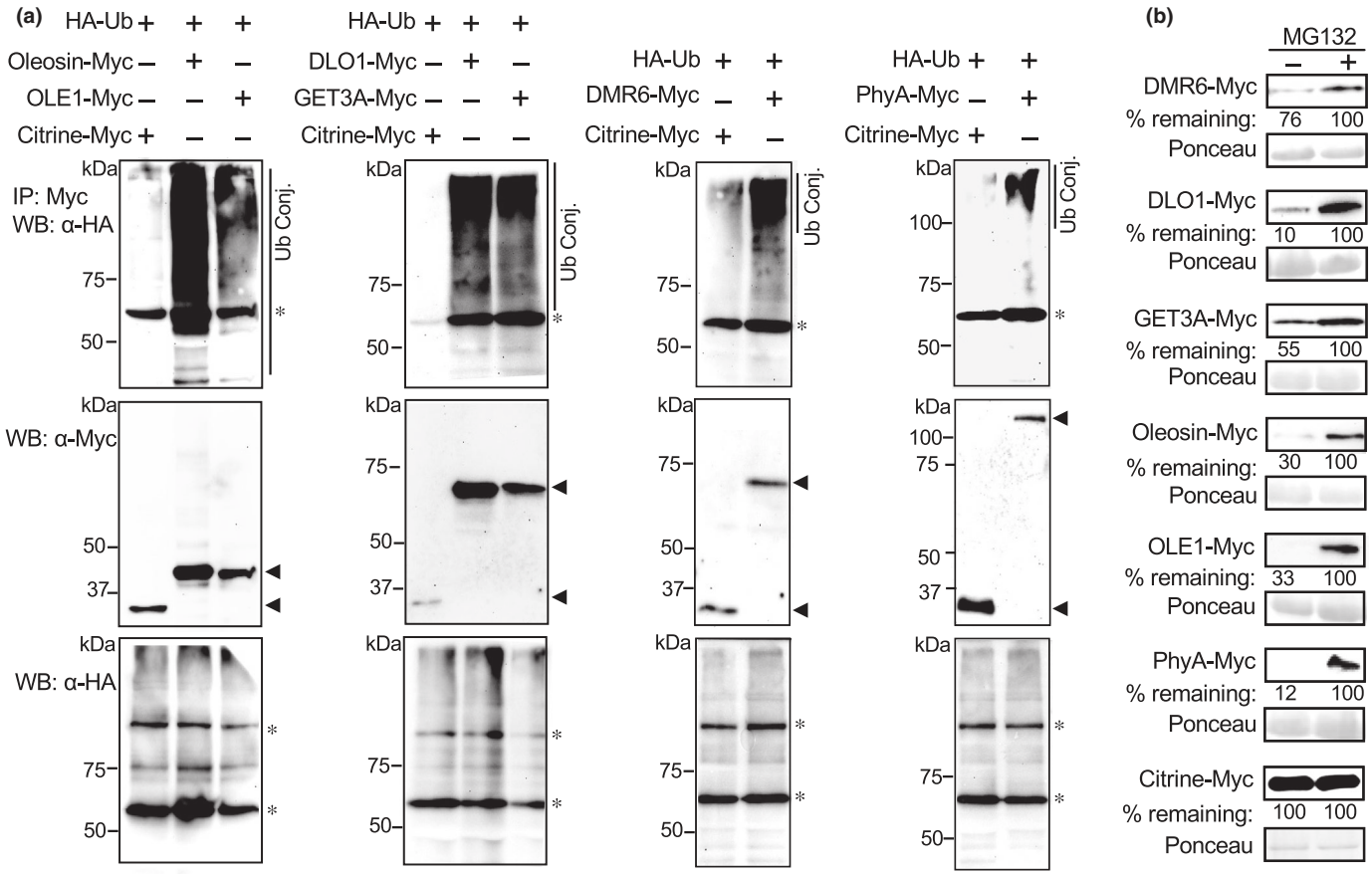

Fig. 3 Identified interactors undergo ubiquitination and proteasomal-dependent degradation. (a) Ubiquitination of targets. Agrobacterium harboring 3xHA-tagged Ubiquitin (HA-Ubiquitin) and 3xMyc-tagged target proteins (target-Myc) or citrine-Myc control were co-infiltrated into *Nicotiana benthamiana* leaves. After 36 h, 50 μM MG132 was infiltrated, and leaf tissues were harvested 12 h later for co-immunoprecipitation. Proteins were immunoprecipitated (IP) with Myc antibody-conjugated agarose beads followed by Western blot (WB) with HA antibody (top panels). Arrows mark the expected target bands on the gel and asterisks indicate nonspecific bands. Molecular weight marker sizes are shown on the left of each blot. (b) Proteasome-dependent degradation of targets. Agrobacterium carrying 3xMyc-tagged target proteins (target-Myc) or citrine-Myc control were infiltrated into *N. benthamiana* leaves. At 36 hours postinfiltration, 50 μM MG132 (+) or DMSO control (−) was added. Twelve hours later, leaf tissues were ground in liquid nitrogen and 2.5× (g ml^{-1}) 2× sample buffer was added directly to the powdered material, followed by boiling for 5 min and immunoblotted with Myc antibody. The percent reduction in protein shown at the bottom of each gel was normalized using a loading control and quantified using the ImageLab software (Bio-Rad).

Discussion

Here, we present the SCF interactome landscape *in planta* and unveil new targets of the ubiquitin system by leveraging an optimized, tightly controlled PL strategy combined with protein interactions, polyubiquitination, and proteasomal degradation. While it has been previously demonstrated that PhyA and OLE1 undergo proteasomal degradation (Clough & Vierstra, 1997; Traver & Bartel, 2023), they have not been specifically linked to SCF ubiquitin ligase complex. It is possible that targets of the ubiquitin system can be regulated by distinct E3 ligase families. For instance, while OLE1 is identified as an SCF target in our study, it has recently been found to undergo ubiquitination mediated by the RING-type E3 MIEL1 (Traver & Bartel, 2023). Hence, it is conceivable that the regulation of OLE1 turnover can be regulated by multiple E3s, potentially dependent on factors such as differential expression or other post-translational modifications, such as phosphorylation. PhyA degradation, a pivotal process in plant photoreceptor regulation, has been regulated by the ubiquitin-proteasome pathway, as evidenced by various recognition domains for ubiquitination (Clough & Vierstra, 1997). Our research proposes an additional targeting mechanism of PhyA involving an SCF-type E3 ligase, and future studies are awaited to further reveal the associated F-box protein. Strikingly, DMR6, DLO1, Oleosin, and GET3A have not been previously shown to undergo ubiquitin-mediated proteasomal degradation. DMR6 and DLO1 were characterized as 2-oxoglutarate (2OG) and Fe(II)-dependent oxygenase superfamily proteins that catalyze the hydroxylation of the defense hormone salicylic acid (SA; Zhang *et al.*, 2017; Zeilmaker *et al.*, 2015). E3-mediated ubiquitination of SA-mediated immunity coactivator NPR1 is critical for mediating SA perception and establishment of systemic acquired resistance (Skelly *et al.*, 2019; Zavaliev *et al.*, 2020). This suggests a link between SCF E3-mediated

ubiquitination and SA inactivation, further solidifying the ubiquitin system as a major player in SA signaling. Gaining further mechanistic insight into the ubiquitin-mediated degradation of DMR6 and DLO1 would have promising implications for crop improvement purposes, as loss-of-function for DMR6 and DLO1 has been shown to increase SA levels and resistance to pathogens (Zeilmaker *et al.*, 2015; Zhang *et al.*, 2017; Thomazella *et al.*, 2021).

Notably, our proxitome profiled a relatively low number of F-box proteins, despite the highly efficient *cis*-biotinylation of ASK1, which serves as an intrinsic control for its expression and biotinylating activity. We can only speculate that the unexpectedly low abundance of F-box proteins might be due to limitations in the experiment's ability to capture some F-box proteins that assemble into SCF complexes during specific developmental stages, in specific tissues, or when plants are exposed to biotic and abiotic stimuli. It is also possible that effective biotinylation is influenced by the availability of exposed lysine residues to which biotin is transferred during PL. Another limitation of the proxitome could be related to our selection of ASK1 as a bait. While the rationale for selecting ASK1 is clearly justified by numerous reports of its prominent activity as an SCF adaptor, it cannot be ruled out that other underexplored ASK proteins, such as ASK2 and ASK11, may participate in the SCF complex and provide additional specificity for F-box selection in certain tissues, under specific environmental stimuli, and at different developmental stages (Gagne *et al.*, 2002; Risseeuw *et al.*, 2003).

Furthermore, it is possible that Arabidopsis ASK1 has dual, non-SCF functions. Recently, mammalian SKP1 has been shown to regulate a switch between autophagy and unconventional protein secretion, suggesting that ASK1 may have biological functions beyond its role as an adaptor protein within the SCF complex (Li *et al.*, 2023). Therefore, the F-box proteins and other proteins we captured under our experimental conditions with ASK1 could represent a snapshot at a specific developmental stage and/or could be part of noncanonical SCF complexes. Further studies utilizing our transgenic lines described here will be valuable for capturing F-box proteins that assemble into SCF complexes and other targets that associate with ASK1 in an SCF-independent complex under various biological conditions.

In summary, our study has revealed numerous novel interactors and substrates of SCF-type ubiquitin ligase, underscoring the pivotal role of these enzymes in upholding homeostasis for facilitating optimal plant growth and development. Our research not only illuminates the SCF interactome landscape but also emphasizes the necessity for further elucidation of the functions of these interacting proteins within relevant biological contexts. Establishing a robust platform for capturing the E3 interactome has the potential to enhance our comprehension of protein turnover regulation through ubiquitination and degradation in response to various biotic and abiotic stressors.

Acknowledgements

NS is supported by the National Science Foundation (NSF-CAREER Award #2047396 and Award #2139805). NS and JWW are supported by the US Department of Energy, Office of Science, Biological and Environmental Research, Genomic Science Program grant no.: DE-SC0023158. NS and SPD-K are supported by NSF-EAGER Award #2028283. SPD-K acknowledges support from the National Institute of Health (NIH) grant R01GM132582 and NSF-IOS Award #2139987. JWW acknowledges support from NSF-IOS-2039489, NSF-IOS-1759023, the US Department of Agriculture (Hatch IOW04108), and the ISU Plant Sciences Institute. NH is supported by the USDA National Institute of Food and Agriculture (USDA-NIFA) predoctoral fellowship grant 009041.

Competing interests

None declared.

Author contributions

NS and SPD-K designed the research. FS and NH performed most of the experiments. YL assisted in cloning, optimization of TurboID assay, and transient expression experiments. NDM performed confocal microscopy. CM performed LC-MS/MS and analysis. CM and JW performed proteomics data analysis and generated interaction networks. FS and NH wrote the original draft of the paper. NS, SPD-K, JW and CM wrote, reviewed, and edited the paper.

ORCID

Savithramma P. Dinesh-Kumar https://orcid.org/0000-0001-5738-316X
Natalie Hamada https://orcid.org/0000-0003-0388-5177
Yuanyuan Li https://orcid.org/0000-0001-8615-4374
Nathan D. Meier https://orcid.org/0000-0003-2312-0059
Christian Montes https://orcid.org/0000-0003-1249-2308
Nitzan Shabek https://orcid.org/0000-0002-2190-5955
Fuai Sun https://orcid.org/0000-0003-4076-661X
Justin W. Walley https://orcid.org/0000-0001-7553-2237

Data availability

Mass spectrometry data can be downloaded from MassIVE (http://massive.ucsd.edu) using the identifier MSV000093959.

Fuai Sun[1], Natalie Hamada[1], Christian Montes[2], Yuanyuan Li[1], Nathan D. Meier[1], Justin W. Walley[2], Savithramma P. Dinesh-Kumar[1,3]* and Nitzan Shabek[1]*

[1]Department of Plant Biology, College of Biological Sciences, University of California, Davis, Davis, CA 95616, USA; [2]Department of Plant Pathology, Entomology, and Microbiology, Iowa State University, Ames, IA 50011, USA; [3]The Genome Center, University of California, Davis, Davis, CA 95616, USA
(*Authors for correspondence: email: nshabek@ucdavis.edu; spdineshkumar@ucdavis.edu)

References

Abd-Hamid N, Ahmad-Fauzi MI, Zainal Z, Ismail I. 2020. Diverse and dynamic roles of F-box proteins in plant biology. *Planta* **251**: 68.

Berardini TZ, Reiser L, Li D, Mezheritsky Y, Muller R, Strait E, Huala E. 2015. The Arabidopsis information resource: making and mining the 'gold standard' annotated reference plant genome. *Genesis* **53**: 474–485.

Bindea G, Mlecnik B, Hackl H, Charoentong P, Tosolini M, Kirilovsky A, Fridman WH, Pagès F, Trajanoski Z, Galon J. 2009. ClueGO: a Cytoscape plug-in to decipher functionally grouped gene ontology and pathway annotation networks. *Bioinformatics* **25**: 1091–1093.

Branon TC, Bosch JA, Sanchez AD, Udeshi ND, Svinkina T, Carr SA, Feldman JL, Perrimon N, Ting AY. 2018. Efficient proximity labeling in living cells and organisms with TurboID. *Nature Biotechnology* **36**: 880–887.

Clark NM, Nolan TM, Wang P, Song G, Montes C, Valentine CT, Guo H, Sozzani R, Yin Y, Walley JW. 2021. Integrated omics networks reveal the temporal signaling events of Brassinosteroid response in Arabidopsis. *Nature Communications* **12**: 5858.

Clough RC, Vierstra RD. 1997. Phytochrome degradation. *Plant, Cell & Environment* **20**: 713–721.

Cox J, Mann M. 2008. MaxQuant enables high peptide identification rates, individualized p.p.b. – range mass accuracies and proteome-wide protein quantification. *Nature Biotechnology* **26**: 1367–1372.

Cox J, Neuhauser N, Michalski A, Scheltema RA, Olsen JV, Mann M. 2011. Andromeda: a peptide search engine integrated into the MaxQuant environment. *Journal of Proteome Research* **10**: 1794–1805.

Dharmasiri N, Dharmasiri S, Weijers D, Lechner D, Yamada M, Hobbie L, Ehrismann JS, Jürgens G, Estelle M. 2005. Plant development is regulated by a family of auxin receptor F box proteins. *Developmental Cell* **9**: 109–119.

Elias JE, Gygi SP. 2007. Target-decoy search strategy for increased confidence in large-scale protein identifications by mass spectrometry. *Nature Methods* **4**: 207–214.

Gagne JM, Downes BP, Shiu SH, Durski AM, Vierstra RD. 2002. The F-box subunit of the SCF E3 complex is encoded by a diverse superfamily of genes in Arabidopsis. *Proceedings of the National Academy of Sciences, USA* **99**: 11519–11524.

Geisler-Lee J, O'Toole N, Ammar R, Provart NJ, Millar AH, Geisler M. 2007. A predicted interactome for Arabidopsis. *Plant Physiology* **145**: 317–329.

Gou M, Su N, Zheng J, Huai J, Wu G, Zhao J, He J, Tang D, Yang S, Wang G. 2009. An F-box gene, CPR30, functions as a negative regulator of the defense response in Arabidopsis. *The Plant Journal* **60**: 757–770.

Harper JW, Tan MK. 2012. Understanding Cullin-RING E3 biology through proteomics-based substrate identification. *Molecular & Cellular Proteomics* **11**: 1541–1550.

Iconomou M, Saunders DN. 2016. Systematic approaches to identify E3 ligase substrates. *Biochemical Journal* **473**: 4083–4101.

Kim D, Roux KJ. 2016. Filling the void: proximity-based labeling of proteins in living cells. *Trends in Cell Biology* **26**: 804–817.

Kruger NJ. 2009. The Bradford method for protein quantitation. In: Walker JM, ed. *The protein protocols handbook*. Totowa, NJ, USA: Humana Press, 17–24.

Kuroda H, Yanagawa Y, Takahashi N, Horii Y, Matsui M. 2012. A comprehensive analysis of interaction and localization of Arabidopsis SKP1-LIKE (ASK) and F-box (FBX) proteins. *PLoS ONE* **7**: e50009.

Lechner E, Achard P, Vansiri A, Potuschak T, Genschik P. 2006. F-box proteins everywhere. *Current Opinion in Plant Biology* **9**: 631–638.

Li J, Krause GJ, Gui Q, Kaushik S, Rona G, Zhang Q, Liang FX, Dhabaria A, Anerillas C, Martindale JL *et al.* 2023. A noncanonical function of SKP1 regulates the switch between autophagy and unconventional secretion. *Science Advances* **9**: eadh1134.

Li J, Witten DM, Johnstone IM, Tibshirani RM. 2012. Normalization, testing, and false discovery rate estimation for RNA-sequencing data. *Biostatistics* **13**: 523–538.

Liang W, Tong M, Li X. 2020. SUSA2 is an F-box protein required for autoimmunity mediated by paired NLRs SOC3-CHS1 and SOC3-TN2. *Nature Communications* **11**: 5190.

Lohmann D, Stacey N, Breuninger H, Jikumaru Y, Müller D, Sicard A, Leyser O, Yamaguchi S, Lenhard M. 2010. SLOW MOTION is required for within-plant auxin homeostasis and normal timing of lateral organ initiation at the shoot meristem in Arabidopsis. *Plant Cell* **22**: 335–348.

Mair A, Xu SL, Branon TC, Ting AY, Bergmann DC. 2019. Proximity labeling of protein complexes and cell-type-specific organellar proteomes in Arabidopsis enabled by TurboID. *eLife* **8**: e47864.

Nakagami H, Soukupová H, Schikora A, Zárský V, Hirt H. 2006. A mitogen-activated protein kinase kinase kinase mediates reactive oxygen species homeostasis in Arabidopsis. *Journal of Biological Chemistry* **281**: 38697–38704.

Nguyen HN, Kim JH, Jeong CY, Hong SW, Lee H. 2013. Inhibition of histone deacetylation alters Arabidopsis root growth in response to auxin via PIN1 degradation. *Plant Cell Reports* **32**: 1625–1636.

Pierce NW, Kleiger G, Shan S, Deshaies RJ. 2009. Detection of sequential polyubiquitylation on a millisecond timescale. *Nature* **462**: 615–619.

Porat P, Lu P, O'Neill SD. 1998. Arabidopsis SKP1, a homologue of a cell cycle regulator gene, is predominantly expressed in meristematic cells. *Planta* **204**: 345–351.

Qin W, Cho KF, Cavanagh PE, Ting AY. 2021. Deciphering molecular interactions by proximity labeling. *Nature Methods* **18**: 133–143.

Risseeuw EP, Daskalchuk TE, Banks TW, Liu E, Cotelesage J, Hellmann H, Estelle M, Somers DE, Crosby WL. 2003. Protein interaction analysis of SCF ubiquitin E3 ligase subunits from Arabidopsis. *The Plant Journal* **34**: 753–767.

Sadanandom A, Bailey M, Ewan R, Lee J, Nelis S. 2012. The ubiquitin–proteasome system: central modifier of plant signalling. *New Phytologist* **196**: 13–28.

Shannon P, Markiel A, Ozier O, Baliga NS, Wang JT, Ramage D, Amin N, Schwikowski B, Ideker T. 2003. Cytoscape: a software environment for integrated models of biomolecular interaction networks. *Genome Research* **13**: 2498–2504.

Skelly MJ, Furniss JJ, Grey H, Wong KW, Spoel SH. 2019. Dynamic ubiquitination determines transcriptional activity of the plant immune coactivator NPR1. *eLife* **8**: e47005.

Song G, Montes C, Walley JW. 2020. Quantitative profiling of protein abundance and phosphorylation state in plant tissues using Tandem mass tags. In: Jorrin-Novo JV, Valledor L, Angeles Castillejo M, Rey MD, eds. *Plant proteomics: methods and protocols*. New York, NY, USA: Springer US, 147–156.

Stefanowicz K, Lannoo N, Van Damme EJM. 2015. Plant F-box proteins – judges between life and death. *Critical Reviews in Plant Sciences* **34**: 523–552.

Teicher BA, Tomaszewski JE. 2015. Proteasome inhibitors. *Biochemical Pharmacology* **96**: 1–9.

Thomazella DPDT, Seong K, Mackelprang R, Dahlbeck D, Geng Y, Gill US, Qi T *et al.* 2021. Loss of function of a DMR6 ortholog in tomato confers broad-spectrum disease resistance. *Proceedings of the National Academy of Sciences, USA* **118**: e2026152118.

Traver MS, Bartel B. 2023. The ubiquitin-protein ligase MIEL1 localizes to peroxisomes to promote seedling oleosin degradation and lipid droplet mobilization. *Proceedings of the National Academy of Sciences, USA* **120**: e2304870120.

Waese J, Provart NJ. 2016. The bio-analytic resource for plant biology. *Plant Genomics Databases* 119–148.

Xu L, Liu F, Lechner E, Genschik P, Crosby WL, Ma H, Peng W, Huang D, Xie D. 2002. The SCFCOI1 ubiquitin-ligase complexes are required for jasmonate response in Arabidopsis. *Plant Cell* **14**: 1919–1935.

Yang M, Hu Y, Lodhi M, McCombie WR, Ma H. 1999. The Arabidopsis SKP1-LIKE1 gene is essential for male meiosis and may control homologue separation. *Proceedings of the National Academy of Sciences, USA* **96**: 11416–11421.

Yang X, Wen Z, Zhang D, Li Z, Li D, Nagalakshmi U, Dinesh-Kumar SP, Zhang Y. 2021. Proximity labeling: an emerging tool for probing *in planta* molecular interactions. *Plant Communications* **2**: 100137.

Zavaliev R, Mohan R, Chen T, Dong X. 2020. Formation of NPR1 condensates promotes cell survival during the plant immune response. *Cell* **182**: 1093–1108.

Zeilmaker T, Ludwig NR, Elberse J, Seidl MF, Berke L, Van Doorn A, Schuurink RC, Snel B, Van den Ackerveken G. 2015. DOWNY MILDEW RESISTANT 6 and DMR6-LIKE OXYGENASE 1 are partially redundant but distinct suppressors of immunity in Arabidopsis. *The Plant Journal* **81**: 210–222.

Zhang Y, Song G, Lal NK, Nagalakshmi U, Li Y, Zheng W, Huang PJ, Branon TC, Ting AY, Walley JW *et al.* 2019. TurboID-based proximity labeling reveals that

UBR7 is a regulator of N NLR immune receptor-mediated immunity. *Nature Communications* **10**: 1–17.

Zhang Y, Zhao L, Zhao J, Li Y, Wang J, Guo R, Gan S, Liu CJ, Zhang K. 2017. S5H/DMR6 encodes a salicylic acid 5-hydroxylase that fine-tunes salicylic acid homeostasis. *Plant Physiology* **175**: 1082–1093.

Zhao D, Yang M, Solava J, Ma H. 1999. The ASK1 gene regulates development and interacts with the UFO gene to control floral organ identity in Arabidopsis. *Developmental Genetics* **25**: 209–223.

Zheng N, Schulman BA, Song L, Miller JJ, Jeffrey PD, Wang P, Chu C, Koepp DM, Elledge SJ, Pagano M *et al.* 2002. Structure of the Cul1–Rbx1–Skp1–F boxSkp2 SCF ubiquitin ligase complex. *Nature* **416**: 703–709.

Zheng N, Shabek N. 2017. Ubiquitin ligases: structure, function, and regulation. *Annual Review of Biochemistry* **86**: 129–157.

Supporting Information

Additional Supporting Information may be found online in the Supporting Information section at the end of the article.

Fig. S1 Uncropped gels and loading controls used in this study.

Fig. S2 TurboID-based proximity labeling design and optimization.

Fig. S3 Correlation between samples used for ASK1 and $CUL1^{NTD}$ proximity labeling experiment.

Fig. S4 Validation of interaction between ASK1 and $CUL1^{NTD}$ with targets.

Table S1 Primers and proximity labeling plasmid sequences used in this study.

Table S2 CUL1 and ASK1 TurboID-based proximity labeling results.

Table S3 ASK1 and CUL1 common interactors.

Table S4 Ub-related genes.

Table S5 List of enriched F-box proteins and substrates.

Table S6 GO analysis details.

Table S7 Ub genes enrichment.

Table S8 Targets for validation.

Please note: Wiley is not responsible for the content or functionality of any Supporting Information supplied by the authors. Any queries (other than missing material) should be directed to the *New Phytologist* Central Office.

Key words: ASK1, CUL1, interactome, proximity labeling, SCF, TurboID, ubiquitin, ubiquitin ligase.

Received, 28 May 2024; accepted, 14 July 2024.